AIMS Mathematics, 11(6): 16635–16671.
DOI: 10.3934/math.2026683
Received: 10 April 2026
Revised: 01 June 2026
Accepted: 02 June 2026
Published: 10 June 2026

https://www.aimspress.com/journal/Math

Research article

TAHO: tri-swarm adaptive hybrid optimizer for optimal power flow in integrated transmission-distribution systems

Tariq Ali[1,2,*], Muzna Sarwar[3,*], Farrukh Jamal[4], Mohammad Hijji[2], Husam S. Samkari[1,5], Mohammed F. Allehyani[5] and Muhammad Ayaz[1,2]

[1] Artificial Intelligence and Sensing Technology Research Center (AIST), University of Tabuk, Tabuk 71491, Saudi Arabia

[2] Faculty of Computers and Information Technology, University of Tabuk, Tabuk 71491, Saudi Arabia

[3] Department of Statistics, Faculty of Computing, Islamia University of Bahawalpur, Pakistan

[4] Department of Statistics, Faculty of Science, University of Tabuk, Tabuk, Saudi Arabia

[5] Department of Electrical Engineering, University of Tabuk, Tabuk 47713, Saudi Arabia

* **Correspondence:** Email: teshaq@ut.edu.sa, muznastatphd@gmail.com.

Abstract: The increasing integration of renewable energy resources and active distribution networks has significantly increased the complexity of optimal power flow (OPF) problems in integrated transmission-distribution (T&D) power systems. To address these challenges, this paper proposes a novel tri-swarm adaptive hybrid optimizer (TAHO) that integrates particle swarm optimization (PSO), grey wolf optimizer (GWO), and jellyfish search (JS) within a unified adaptive optimization framework. The proposed method effectively balances exploration and exploitation to improve convergence stability and optimization accuracy. A multi-objective OPF model is developed to minimize generation cost, power loss, and voltage deviation under operational constraints. Experimental results on integrated IEEE 30-bus and IEEE 33-bus systems demonstrate that the proposed TAHO achieves superior performance with the minimum fitness value of 0.0008, faster convergence within 75 iterations, and the lowest standard deviation of 0.0005 compared with PSO, GWO, and JS. Benchmark evaluations further confirm the robustness and strong global search capability of the proposed framework for renewable-integrated smart grid optimization and real-time OPF applications.

Keywords: optimal power flow; hybrid metaheuristic optimization; distribution systems; renewable energy integration; power system
Mathematics Subject Classification: 34A08, 68T07

1. Introduction

The global transition toward low-carbon energy systems has accelerated the integration of renewable energy resources, distributed generation (DG), and energy storage technologies into modern power networks. This shift is leading to a fundamental change in how power systems are structured. Traditional power systems were built to accommodate large-scale central generation and unidirectional power flow. However, with the continued growth of distributed energy resources, power systems are shifting toward a more distributed and grid-like topology where transmission and distribution networks are highly interconnected and must operate collaboratively. Operation of power networks becomes more complex as they become increasingly interconnected with features like bidirectional power flows, renewable intermittency, and distributed energy resource fleet dynamics. The optimal power flow (OPF) problem is becoming increasingly important for managing the operation of power networks to ensure secure, reliable, and cost effective operation.

Traditionally, transmission and distribution systems were studied and optimized independently. However, with the rapid growth of DG and active distribution networks, this separation is no longer sufficient. Integrated transmission-distribution (T&D) system modeling has therefore become an active research area to better represent interactions between multiple layers of the power network [1]. Authors of [2] discussed decentralized stochastic optimization for planning integrated T&D networks with high penetration of DG. As power systems become more complicated with high penetrations of renewable and DGs advanced optimization approaches are needed to coordinate operations of these systems. Toward this end, authors in [3] presented a detailed review of integrated T&D system modeling. More recently, authors in [4] proposed a multi-timescale scheduling framework for transmission and distribution networks with high renewable penetration, demonstrating the necessity of coordinated risk-aware optimization strategies.

The OPF problem plays a central role in the operation and planning of power systems, as it aims to determine the optimal operating point of generators and control devices while satisfying physical and operational constraints of the network. However, solving the OPF problem in integrated T&D systems is significantly more challenging than in conventional transmission networks. There are numerous reasons for this complexity such as non-linear power flow equations, the interaction of extensive systems, uncertainty of distributed generations, etc. authors in [5] proposed interval power flow for an integrated T&D system to handle the issues discussed above. Authors in [6] also presented distributed optimization-based system restoration for integrated transmission and distribution systems. However, there are limited methods to solving OPF problems quickly for large-scale integrated power networks. To solve OPF problems various mathematical optimization techniques and computational intelligence-based algorithms have been investigated. Traditional optimization methods like linear programming, nonlinear programming, and interior-point methods have been used extensively in solving optimization problems in power systems. However, they become inefficient when dealing with large-scale and complex highly nonlinear nonconvex multi-modal optimization problems. Consequently, metaheuristic optimization algorithms have gained increasing attention due to their ability to explore complex search spaces without requiring gradient information.

Various works have addressed optimization issues on power systems with metaheuristic approaches. The authors in [7] presented a hybrid moth-flame and particle swarm optimization (PSO) metaheuristic to address power system optimization problems and proved its better convergence

properties than classical methods. Authors in [8] focused on reactive power optimization for distribution networks with high penetration of renewable energy sources (RESs) to obtain voltage support and minimize power losses with intelligent optimization algorithms. Optimal scheduling of distribution networks with high penetration of DG and energy storage systems (ESSs) was presented in [9]. Other studies regarding optimization issues on modern power systems have included evolutionary algorithms, robust optimization formulation, and distributed coordination [10]. Recently, a few researchers have looked into the newly intelligent optimization algorithms such as reinforcement learning algorithms, generative models, and hybrid evolutionary algorithms to solve different electrical optimization problems due to complexity growth in smart grids. Authors in [11] developed a generative adversarial network (GAN) based robust optimization approach for the distribution network planning problem, and [12] presented a jellyfish search (JS)-based optimization method for the reactive power dispatch problem. Furthermore, a survey paper was presented on grey wolf optimizer (GWO) along with its applications in energy-related sectors, which was found to be effective for nonlinear optimization problems [13]. Similarly, very recent articles on reinforcement learning algorithms [14] and hybrid algorithms have been applied for electrical network optimization problems. However, most of the available meta-heuristic algorithms follow the single optimization paradigm, which leads to inadequate global search as well as local exploitation abilities.

The other trend is to apply a control and optimization framework into active distribution networks/smart grids. Several papers discussed distributed coordination and energy management in active networks recently. Authors in [15] discussed distributed the source–load–storage coordination framework for active distribution networks. Reference [16] analyzed flexibility aggregation of DG and energy storage community. Furthermore, a blockchain-based energy trading mechanism was introduced into electrical power systems to enable decentralized energy market and transparency [17]. While these methods can be considered as promising methods for future smart grids, it still needs efficient optimization algorithms to handle the complex operations of T&D integrated systems.

Existing optimization techniques still face significant challenges when solving nonlinear and nonconvex OPF problems in renewable-integrated T&D systems. Conventional metaheuristic algorithms such as PSO, GWO, and JS often suffer from premature convergence, weak exploration-exploitation balance, and limited robustness in large-scale smart grid environments. To overcome these limitations, this study proposes a novel tri-swarm adaptive hybrid optimizer (TAHO) that integrates PSO, GWO, and JS within a unified adaptive optimization framework. The proposed method dynamically balances global exploration and local exploitation using an adaptive weighted search mechanism to improve convergence stability, optimization accuracy, and search diversity. A multi-objective OPF formulation is developed to simultaneously minimize generation cost, transmission loss, and voltage deviation. Experimental results on integrated IEEE 30-bus and IEEE 33-bus systems demonstrate that the proposed TAHO achieves superior performance with the minimum fitness value of 0.0008, faster convergence within 75 iterations, and the lowest standard deviation of 0.0005 compared with conventional optimization methods. Benchmark evaluations further confirm the robustness and strong global search capability of the proposed framework for renewable-integrated smart grid optimization and real-time OPF applications.

The main contributions of this study can be summarized as follows:

- A novel hybrid metaheuristic optimization algorithm, termed the TAHO, is developed by integrating PSO, GWO, and JS mechanisms to improve search diversity and convergence

performance.

- A coordinated OPF framework for integrated T& D systems is formulated considering generation cost, transmission losses, and voltage deviation minimization under operational constraints.
- The proposed hybrid optimization strategy enhances the balance between exploration and exploitation, reducing the risk of premature convergence commonly observed in conventional metaheuristic algorithms.
- Extensive simulations demonstrate the effectiveness and robustness of the proposed TAHO algorithm in solving complex OPF problems in renewable-integrated power systems.

The remainder of this paper is organized as follows. Section 2 describes the mathematical formulation of the OPF problem in integrated T&D systems. Section 3 presents the proposed TAHO and its algorithmic framework. Section 4 discusses the simulation setup and experimental results. Finally, Section 5 concludes the paper and outlines future research directions.

2. Literature review

The high penetration of RES, DGs, and ESSs has fundamentally changed the architecture of the existing power systems. While conventional power systems were operated considering centralized generation and unidirectional power flow, smart grids necessitate the operation of transmission and distribution networks in a coordinated manner. Hence, T&D system optimization is gaining more attention to improve the overall efficiency, reliability, and flexibility of power systems. An overview of various optimization techniques along with their limitations is summarized in Table 1. Some of the earlier efforts were directed toward coordinated planning and modeling of integrated T&D networks. Stochastic optimization formulations were proposed for integrated T&D planning under high DG penetration [2], and modeling studies for the coupled network highlighted the necessity of coordinated operation of the overall system [18]. Multi-timescale scheduling techniques were proposed to incorporate risk-aware scheduling of large-scale integrated networks [4]. Interval power flow and distributed optimization techniques were employed to address uncertainty and system restoration in integrated T&D systems [19, 20].

Even though these techniques provide a better modeling of the system, they result in higher computation complexity and communication burden. In addition to T&D system operation, different optimization frameworks are implemented to improve power system operation at the distribution level. Optimization methods of reactive power are conducted for voltage regulation [21], and energy scheduling optimization was applied to dispatch DG and storage units [22]. Two-stage optimization formulations were designed for energy markets [23], while robust optimization was adopted to tackle network resilience [24]. Methods ranging from service restoration to blockchain-technology based energy trading are also proposed to optimize smart grid resiliency and decentralization [25, 26]. Many of these solutions are limited to single paradigms of optimization and lack scalability and integration with T&D systems.

Table 1. Comparison of existing optimization studies in transmission and distribution networks.

Reference	Method	Application	Network type	Limitation
[2]	Stochastic optimization	T&D planning with DG	Integrated T&D	High computational cost
[18]	System modeling review	T&D modeling	Integrated networks	Lack of optimization strategy
[4]	Multi-timescale scheduling	Risk-aware scheduling	T&D networks	Limited scalability
[19]	Interval power flow	Uncertainty analysis	Integrated networks	High model complexity
[20]	Distributed optimization	System restoration	T&D networks	Communication overhead
[7]	Hybrid MFO-PSO	Power optimization	T&D networks	Premature convergence
[21]	Reactive power optimization	Voltage control	Distribution	Limited integration with T&D
[22]	Energy scheduling	DG and storage management	Distribution	Single optimization method
[23]	Two-stage optimization	Energy markets	T&D networks	High computational complexity
[24]	Robust optimization	Multistage resilience	Distribution	Limited scalability
[25]	Service restoration	Network recovery	Distribution	Limited optimization scope
[26]	Blockchain framework	Energy trading	Smart grids	High implementation cost
[11]	GAN-based optimization	DG planning	Distribution	Model training complexity
[12]	Jellyfish search (JS)	Reactive power dispatch	Transmission	Limited hybrid capability
[13]	Grey wolf optimization	Energy systems	Transmission	Slow convergence
[27]	Stackelberg game model	PV energy sharing	Distribution	Limited scalability
[28]	Intelligent fault detection	Active networks	Distribution	Limited optimization analysis
[29]	Grasshopper optimization	Data transmission systems	Smart systems	Limited energy modeling
[30]	Active network management	Expansion planning	Distribution	Lack of optimization framework
[31]	DQN-GA hybrid algorithm	Transmission optimization	Transmission	High training cost
[32]	Smart grid optimization	Energy management	Smart grids	Limited OPF focus
[33]	Flexibility aggregation	Energy storage coordination	Distribution	Limited hybrid optimization
[34]	Multi-objective PSO	Capacitor placement	Distribution	Limited convergence stability

OPF problems are non-linear and non-convex; therefore, to obtain a suitable solution to these problems, metaheuristic optimization algorithms have been applied. Authors in [7] presented a hybrid

moth–flame algorithm and PSO for OPF. A JS algorithm was used for reactive power dispatch in [12]. GWO was applied to solve optimization problems in energy systems because of its excellent performance in terms of global optimization ability in [13]. Multi-objective PSO was utilized for capacitor placement in distribution networks in [14]. These algorithms have low premature convergence and weak global search capabilities. There were recently conducted studies on this topic as well. Intelligent optimization using generative adversarial network (GAN)-based approaches were proposed for DG planning [11]. Game-theoretic based approaches employed to propose Stackelberg framework for sharing of photovoltaic energy [27]. Intelligent Firefly Algorithm strategies were also proposed for active distribution network (ADNs) [28]. The grasshopper optimization algorithm [29], active network management [30], and hybrid RL-based approaches such as deep Q-network-genetic algorithm (DQN-GA) [31] have also been explored. Recently, smart grid optimization frameworks [32] and flexibility aggregation approaches [33] were proposed to coordinate distributed energy resources. Authors in [34] developed a multi-objective PSO-based optimization approach for capacitor bank placement in distribution networks to improve energy efficiency and reduce operational cost.

Recent developments in intelligent optimization and adaptive control approaches have been witnessed with an incorporation of model learning, reinforcement learning, and data-driven optimization methodologies for enhancing their adaptability and decision-making capabilities in nonlinear systems. In particular, reinforcement learning-enhanced control approaches [35] and model- and data-driven optimization approaches [36] have shown improved convergence performance, robustness, and adaptability in challenging engineering applications. Inspired by recent developments, the suggested TAHO approach incorporates an adaptive cooperative hybrid optimization method utilizing PSO, GWO, and JS methods. The adaptive weighting and cooperative search strategies employed by the suggested TAHO method enhance global and local search capabilities, leading to enhanced convergence, robustness, and diversification in optimization tasks for nonlinear OPF problems in renewable-energy- integrated transmission-distribution networks.

In recent times, there has been notable success in the development of hybrid optimisation algorithms for OPF. Authors in [37] proposed a hybrid optimization algorithm that incorporates RES and electric vehicles, thus offering superior performance for OPF problems in the case of multi-objective optimization. Authors in [38] proposed an advanced form of the weighted mean of vectors (WMV) algorithm for dealing with renewable energy uncertainties in hybrid wind-solar-thermal power systems, thereby achieving better solutions for OPF problems under uncertain conditions. Authors in [39] presented different metaheuristics for OPF problems, emphasizing the efficiency of hybrid optimization algorithms.

In [40], an algorithm that combined differential evolution and harris hawks optimization (HHO) techniques was employed to solve the problem of energy management in a microgrid, leading to enhanced stability and reduced costs. In [41], an effective intuitionistic fuzzy environment was introduced for the development of emergency response plans when faced with uncertainties related to disaster risks. Through the combination of fuzzy and intuitionistic fuzzy theories, uncertainties associated with disasters can be handled effectively, making decision-making procedures more efficient. By incorporating the element of uncertainty in risk assessment and planning, this technique presents itself as an effective way of optimizing decisions.

Several hybrid metaheuristic frameworks have been proposed for power system optimization,

including PSO-GWO, PSO-GA, MFO-PSO, and reinforcement-learning-assisted adaptive hybrid optimizers. These approaches have demonstrated improved convergence behavior, solution diversity, and exploration-exploitation balance compared with conventional standalone optimization methods. For instance, hybrid elite learning and Meta-Lamarckian strategies were incorporated into coyote optimization algorithms to enhance multi-objective OPF performance, while PSO-GWO-based hybrid frameworks showed strong robustness and convergence stability in complex nonlinear engineering optimization problems [42, 43]. Furthermore, advanced multi-criteria and hybrid soft-computing optimization frameworks have been developed to address non-convex and highly constrained economic dispatch and OPF problems under uncertainty, achieving improved computational efficiency and global search capability [44, 45]. Many existing hybrid approaches primarily rely on two-algorithm fusion or fixed operator scheduling mechanisms, which may restrict adaptive coordination among exploration, exploitation, and diversity preservation processes during optimization. This limitation motivates the proposed TAHO framework, which integrates three complementary search behaviors within a unified adaptive weighting strategy to enhance convergence stability, population diversity, and global optimization performance.

However, several important problems remain to be addressed. First, most of the work is performed on transmission or distribution networks- but not on the complete T&D network considered together. Second, the majority of approaches use only one type of optimization method, which makes the algorithm biased toward exploration or exploitation and suffers from premature convergence or local optimal solutions. Finally, the majority of the state-of-the-art techniques are computationally intensive or involve training costs, which constrain their application in real-time operation in the current smart grid environment. This study introduces a new metaheuristic hybrid optimization technique "TAHO", which is a perfect combination of the PSO, GWO, and JS techniques. The proposed technique improves the exploration and exploitation abilities and offers a robust solution for solving OPF problems in T&D power systems.

3. Data preprocessing

This section describes the dataset used in this study and the preprocessing procedures applied before implementing the proposed optimization framework. The data preparation stage is essential to ensure numerical stability, accurate power flow modeling, and efficient performance of the proposed TAHO.

3.1. Power system dataset

The benchmark dataset of power systems representing the integrated T&D systems is used to validate the performance of the proposed optimization framework. Detailed and realistic network data are needed for power system studies today to realistically assess OPF algorithms for operation under practical conditions. Standard power system test cases including bus data, line impedance, generator limits, and load demands compose the dataset implemented for this study. In this study, IEEE 30-bus transmission system and IEEE 33-bus radial distribution system are utilized to represent the integrated T&D systems.

Each bus in the system contains information regarding voltage magnitude, active power demand, and reactive power demand. Transmission lines are defined through resistance, reactance, and line charging parameters. The electrical connectivity of the network is represented through the bus

admittance matrix Y_{bus}, which is calculated as

$$Y_{bus} = G + jB, \tag{3.1}$$

where G and B are the conductance and susceptance matrices of the network. This represents the network relationship of the buses that are connected through the transmission and distribution network. This dataset includes DG and renewable energy source models in the distribution network portion along with the typical generation sources. These resources represent modern smart grid environments where distributed energy resources contribute significantly to system operation.

3.2. Per-unit system conversion

Before optimization and power flow calculations are done, all quantities are put in per-unit. Representing system parameters in per-unit simplifies numerical computations involved in power system calculations of large networks.

The per-unit value of a quantity is calculated as

$$X_{pu} = \frac{X_{actual}}{X_{base}}, \tag{3.2}$$

where X_{actual} represents the actual electrical value and X_{base} denotes the corresponding base value of the system. For power systems, base values are typically defined as

$$Z_{base} = \frac{V_{base}^2}{S_{base}}, \tag{3.3}$$

where V_{base} is the base voltage and S_{base} is the base apparent power.

Using the per-unit system improves numerical stability and allows consistent representation of electrical variables across different voltage levels of the integrated T&D network.

3.3. Load and renewable data processing

Load demand data and renewable generation outputs are processed to represent realistic operating conditions of modern power systems. Renewable energy resources such as solar photovoltaic and wind generation introduce variability and uncertainty into the power network. The RESs and DG are not always identical, since DG may include both renewable and conventional distributed sources. In the current formulation, the uncertainty associated with renewable-based DG units can be incorporated by modeling the DG term as a stochastic variable:

$$P_{DG,i} = \bar{P}_{DG,i} + \Delta P_{RES,i}, \tag{3.4}$$

where $\bar{P}_{DG,i}$ represents the forecasted DG power and $\Delta P_{RES,i}$ denotes the uncertainty component caused by renewable intermittency such as solar irradiance and wind speed variations. This formulation enables the OPF model to capture renewable generation uncertainty within the DG framework.

The net injected power at each bus can therefore be expressed as

$$P_i^{net} = P_{gi} + P_{DG,i} - P_{di}, \tag{3.5}$$

where P_{gi} is the conventional generator output, $P_{DG,i}$ represents DG power, and P_{di} denotes the load demand at bus i.

Similarly, the reactive power injection is given by

$$Q_i^{net} = Q_{g,i} + Q_{DG,i} - Q_{L,i}^{net}, \tag{3.6}$$

where $(Q_{L,i}^{net})$ may be positive for inductive loads and negative for capacitive loads. These formulations allow the OPF model to capture the operational impact of DG and renewable energy penetration in the distribution network.

To incorporate ESS into the OPF formulation, the active power balance can be extended as

$$P_i^{net} = P_{gi} + P_{DG,i} + P_{ESS,i}^{dis} - P_{ESS,i}^{ch} - P_{di}, \tag{3.7}$$

where $P_{ESS,i}^{dis}$ and $P_{ESS,i}^{ch}$ represent ESS discharging and charging power, respectively. During discharging, the ESS behaves as a generator, while during charging, it operates as a load. The ESS operation is constrained by charging/discharging limits and state-of-charge (SOC) constraints:

$$SOC_i^{min} \leq SOC_i(t) \leq SOC_i^{max}. \tag{3.8}$$

This modification enables the OPF framework to model bidirectional ESS behavior for improving renewable integration and smart grid operational flexibility.

3.4. Integrated transmission-distribution grid model

In this study, the T&D power systems are coupled at the boundary nodes where power is exchanged between the two networks. The coupling is modeled by considering the active and reactive power flows at these boundary nodes. The power flow is constrained by the following limits:

$$P_{T\to D} \leq P_{T\to D}^{max}, \quad Q_{T\to D} \leq Q_{T\to D}^{max}, \tag{3.9}$$

where $P_{T\to D}$ and $Q_{T\to D}$ represent the active and reactive power flows from the transmission to the distribution system, respectively. Voltage regulation is handled through the coordination of both systems at the boundary, ensuring stable voltage profiles. The energy exchange between the systems is adjusted based on renewable generation and load, with the following power balance:

$$P_{boundary} = P_{T\to D} + P_{DG} - P_{Load}, \tag{3.10}$$

where P_{DG} is the DG power and P_{Load} is the power demand. These interactions and constraints help model the integrated operation of the T&D systems, which is essential for the OPF problem in renewable-integrated grids.

3.5. Construction of network matrices

To facilitate efficient computation during optimization, system variables and constraints are organized into structured matrices representing network topology and electrical connectivity. The bus admittance matrix Y_{bus} plays a critical role in power flow calculations and is used to determine active and reactive power injections at each bus.

The active power balance equation at bus i can be expressed as

$$P_i = V_i \sum_{j=1}^{N_b} V_j(G_{ij}\cos\theta_{ij} + B_{ij}\sin\theta_{ij}). \tag{3.11}$$

Similarly, the reactive power balance equation is defined as

$$Q_i = V_i \sum_{j=1}^{N_b} V_j(G_{ij}\sin\theta_{ij} - B_{ij}\cos\theta_{ij}), \tag{3.12}$$

where V_i and V_j represent voltage magnitudes at buses i and j, and θ_{ij} denotes the phase angle difference.

3.6. Definition of optimization search space

Before applying the proposed optimization algorithm, the feasible search space of decision variables is defined according to system operating limits. Generator active power limits, reactive power limits, and voltage magnitude constraints determine the permissible boundaries of candidate solutions.

The generator operating limits are defined as

$$P_{gi}^{min} \le P_{gi} \le P_{gi}^{max}, \tag{3.13}$$

$$Q_{gi}^{min} \le Q_{gi} \le Q_{gi}^{max}. \tag{3.14}$$

In the initial formulation, $P_{DG,i}$ was treated as a predefined DG input; therefore, explicit operational limits were not included. However, in practical OPF implementation, DG units should also satisfy generation capacity constraints, which can be expressed as

$$P_{DG,i}^{min} \le P_{DG,i} \le P_{DG,i}^{max}. \tag{3.15}$$

This constraint ensures that DG units operate within permissible generation limits under renewable-integrated operating conditions.

Similarly, voltage magnitude limits at each bus are given by

$$V_i^{min} \le V_i \le V_i^{max}. \tag{3.16}$$

These constraints define the feasible region for the OPF problem and guide the search process of the hybrid metaheuristic optimizer.

The variable P_{gi} represents the active power generated at bus i, while Q_{gi} denotes the reactive power generated at the same bus. The term $P_{DG,i}$ refers to the active power generated by DG at bus i. Additionally, P_{loss} represents the total active power loss in the system, and V_i signifies the voltage magnitude at bus i.

3.7. Preparation for hybrid optimization

After completing the preprocessing stage, the processed dataset is used as input to the proposed optimization framework. The TAHO, which integrates PSO, GWO, and JS, iteratively updates

candidate solutions to determine the optimal operating point of the integrated transmission-distribution network.

The preprocessing steps mentioned above normalize system variables, formulate network parameters and define the feasible bounds for optimization. These steps enhance computational efficiency and numerical stability of the proposed hybrid optimization algorithm when employed to solve OPF in renewable-integrated power systems. Figure 1 outlines the preprocessing workflow involved in preparing benchmark T&D network data, which include per-unit conversion of network parameters, incorporation of renewable generation/injection data, network matrix building, and defining optimization bounds prior to application of the proposed hybrid optimization algorithm.

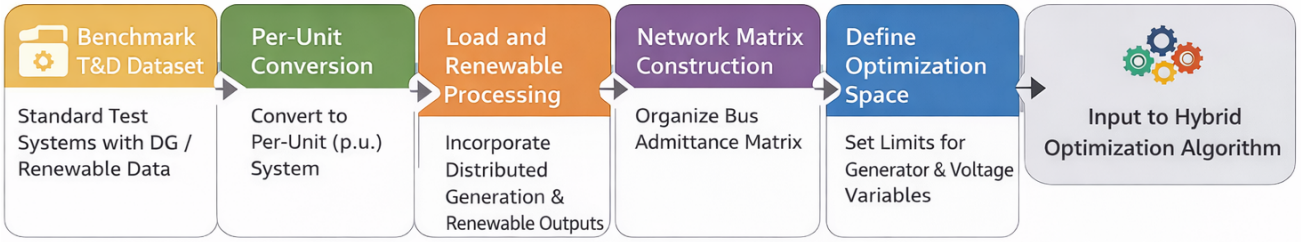

Figure 1. Preprocessing workflow for OPF optimization in integrated transmission-distribution networks.

4. Methodology

This section presents the mathematical modeling of the OPF problem and the architecture of the proposed hybrid optimization framework, TAHO. The OPF problem computes the optimal point of operation for a power system based on specified objectives under network constraints. However, the OPF problem gets involved with additional complexities such as nonlinear power flow equations, renewable energy resource models, and system-wide interactions in contemporary, smart, and fully-integrated T&D systems. Therefore, this study presents a hybrid metaheuristic optimization framework that synergistically integrates three swarm-based algorithms including PSO, GWO, and JS. The advantages of hybridizing these complementary optimization methods include higher convergence stability and better trade-off between exploration and exploitation phases of search.

4.1. OPF problem formulation

The OPF problem is used to find the optimal value of control variables such as generator outputs, voltage magnitudes, and reactive power injections subject to system constraints. The objective function of the OPF model is defined as minimizing the total generation cost while operating the system securely. The generation cost function is given by

$$F_{cost} = \sum_{i=1}^{N_g} (a_i P_{gi}^2 + b_i P_{gi} + c_i), \tag{4.1}$$

where N_g represents the number of generators, P_{gi} denotes the active power output of generator i, and a_i, b_i, and c_i are cost coefficients of the generator.

In addition to generation cost minimization, transmission losses and voltage deviations are also considered to improve overall network efficiency. The active power transmission loss can be calculated as

$$P_{loss} = \sum_{k=1}^{N_l} g_k \left(V_i^2 + V_j^2 - 2V_i V_j \cos(\theta_{ij}) \right), \tag{4.2}$$

where N_l represents the number of transmission lines, g_k is the conductance of line k, and V_i and V_j are bus voltages at the corresponding nodes.

Voltage profile improvement is incorporated through the voltage deviation function

$$F_{volt} = \sum_{i=1}^{N_b} |V_i - V_i^{ref}|, \tag{4.3}$$

where N_b is the number of buses and V_i^{ref} represents the reference voltage magnitude.

The weighting coefficients w_1, w_2, and w_3 satisfy the condition $w_1 + w_2 + w_3 = 1$. The term P_{loss} represents the total active power loss in the system, while F_{cost} denotes the total generation cost. Additionally, F_{volt} refers to the total voltage deviation from the desired profile.

The combined objective function of the OPF problem is formulated as

$$F = w_1 F_{cost} + w_2 P_{loss} + w_3 F_{volt}, \tag{4.4}$$

where w_1–w_3 are the weighting coefficients satisfying $w_1 + w_2 + w_3 = 1$.

The fitness value mentioned in this research work refers to the normalized weighted objective function, wherein the cost (F_{cost}), power loss (P_{loss}), and voltage deviation (F_{volt}) components are normalized and then added. The fitness value calculated to be 0.0008 is not an indication that F_{cost} tends towards zero. Instead, it indicates that the proposed TAHO framework achieves the best overall trade-off among all normalized objective terms while satisfying operational constraints.

The normalized objective function is expressed as

$$F = w_1 \frac{F_{cost}}{F_{cost}^{max}} + w_2 \frac{P_{loss}}{P_{loss}^{max}} + w_3 \frac{F_{volt}}{F_{volt}^{max}}. \tag{4.5}$$

The corresponding optimized objective components obtained using the proposed TAHO framework are approximately:

$$F_{cost} = 803.2 \ \$/h, \tag{4.6}$$

$$P_{loss} = 6.87 \ MW, \tag{4.7}$$

$$F_{volt} = 0.039 \ p.u. \tag{4.8}$$

Thus, the reported fitness value represents the overall normalized multi-objective optimization performance rather than the absolute value of any individual objective component.

4.2. System constraints

The OPF problem must satisfy several equality and inequality constraints that ensure physical feasibility and operational security of the power system.

The equality constraints represent the active and reactive power balance equations at each bus

$$P_{gi} - P_{di} = V_i \sum_{j=1}^{N_b} V_j(G_{ij}\cos\theta_{ij} + B_{ij}\sin\theta_{ij}), \tag{4.9}$$

$$Q_{gi} - Q_{di} = V_i \sum_{j=1}^{N_b} V_j(G_{ij}\sin\theta_{ij} - B_{ij}\cos\theta_{ij}), \tag{4.10}$$

where P_{di} and Q_{di} represent active and reactive power demand, and G_{ij} and B_{ij} are elements of the bus admittance matrix.

The inequality constraints ensure that system variables remain within their operational limits:

$$P_{gi}^{min} \le P_{gi} \le P_{gi}^{max}, \tag{4.11}$$

$$Q_{gi}^{min} \le Q_{gi} \le Q_{gi}^{max}, \tag{4.12}$$

$$V_i^{min} \le V_i \le V_i^{max}, \tag{4.13}$$

$$S_{ij} \le S_{ij}^{max}, \tag{4.14}$$

where V_i^{min} and V_i^{max} are the minimum and maximum allowable voltages at bus i, respectively. These constraints guarantee safe operation of generators, transmission lines, and bus voltages in the integrated T&D network, and P_{gi}^{min} is the minimum active power output of the generator at bus i, representing the lower limit on the amount of active power that a generator can produce. P_{gi}^{max} is the maximum active power output of the generator at bus i, representing the upper limit on the amount of active power that a generator can produce. Q_{gi}^{min} is the minimum reactive power output of the generator at bus i, representing the lower limit on the amount of reactive power that a generator can inject into the system. Q_{gi}^{max} is the maximum reactive power output of the generator at bus i, representing the upper limit on the amount of reactive power that a generator can inject into the system.

4.3. PSO

The PSO is a population-based optimization technique that simulates the social behavior of bird flocks. Each candidate solution is represented as a particle that moves within the search space by adjusting its velocity and position according to its own experience and the experience of neighboring particles. The velocity and position updates are defined as

$$v_i^{t+1} = \omega v_i^t + c_1 r_1(p_{best} - x_i^t) + c_2 r_2(g_{best} - x_i^t), \tag{4.15}$$

$$x_i^{t+1} = x_i^t + v_i^{t+1}, \tag{4.16}$$

where x_i and v_i represent the position and velocity of particle i, p_{best} is the personal best solution, and g_{best} is the global best solution found by the swarm.

4.4. GWO

The GWO mimics social hierarchy and hunting strategy of grey wolves in nature. The candidate solutions are categorized as alpha, beta, and delta wolves, which direct other search agents toward the potential hunting region. Updating of positions are simulated by

$$\vec{D} = |\vec{C} \cdot \vec{X}_p - \vec{X}|, \tag{4.17}$$

$$\vec{X}(t+1) = \vec{X}_p - \vec{A} \cdot \vec{D}, \tag{4.18}$$

where $\vec{A}$ and $\vec{C}$ are coefficient vectors controlling exploration and exploitation during the search process.

4.5. JS Algorithm

The JS algorithm replicates the movement of jellyfish within ocean current motion and swarm movements. Exploration is performed with jellyfish using ocean current movement, while exploitation is completed with swarm behavior. The equation used to update jellyfish position is

$$X_i^{t+1} = X_i^t + \beta(X_{best} - X_i^t), \tag{4.19}$$

where β represents the exploration factor, which controls the global search behavior of the jellyfish swarm, and X_{best} represents the best solution obtained in the current iteration.

4.6. Proposed TAHO

TAHO is proposed based on the strengths of the PSO, GWO, and JS algorithms. All these algorithms are embedded within a single optimization environment. This enables the optimizer to utilize both exploitation and exploration strategies to evade becoming trapped at local optima. Initially, PSO is used to search globally for potential solutions, followed by GWO to enhance candidate solutions through a layered leadership hierarchy. The JS algorithm is used to increase diversity within the population and avoid convergence stagnation through swarm adaptability.

The hybrid position update of the proposed optimizer can be expressed as

$$X_i^{t+1} = \alpha X_{PSO} + \beta X_{GWO} + \gamma X_{JS}, \tag{4.20}$$

where X_{PSO}, X_{GWO}, and X_{JS} represent candidate solutions generated by each optimization strategy, and α, β, and γ are adaptive weights. α is the weighting coefficient for the PSO component. It determines how much influence the PSO algorithm will have on the new solution X_i^{t+1}. β is the weighting coefficient for the GWO component. It defines how much influence the GWO algorithm will have on the new solution. γ is the weighting coefficient for the JS component. It determines how much influence the JS algorithm will have on the new solution

$$\alpha + \beta + \gamma = 1. \tag{4.21}$$

By utilizing this hybrid approach, the proposed TAHO algorithm achieves a balance between global exploration and local exploitation behavior, allowing it to converge quickly to the optimum solution of the OPF problem in the integrated T&D power system. The overall workflow of the proposed TAHO for solving the OPF problem in integrated T&D systems is illustrated in Figure 2. The optimization process begins with the initialization of a population of candidate solutions representing the control variables of the OPF problem, including generator outputs, voltage magnitudes, and reactive power injections. After initialization, the fitness of each candidate solution is evaluated using the objective function, which considers generation cost minimization, power loss reduction, and voltage profile improvement.

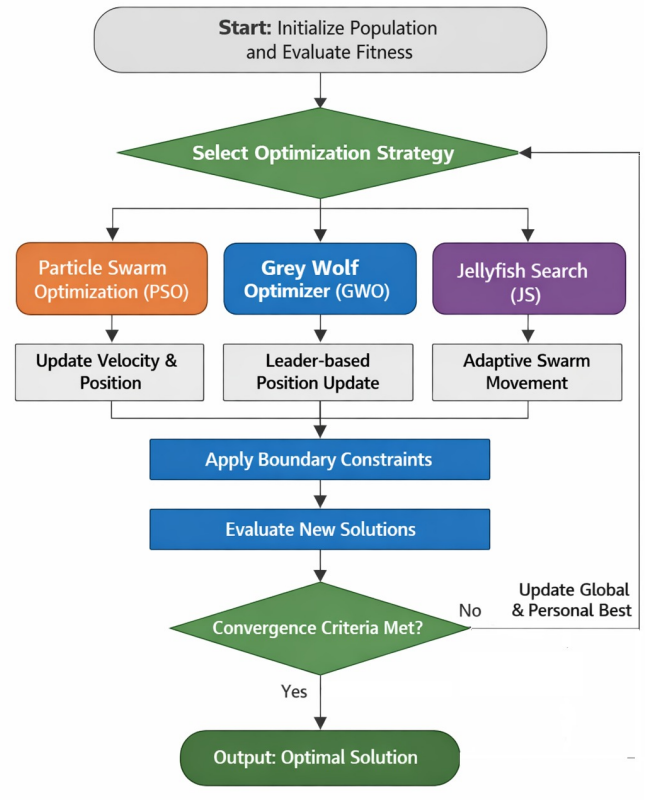

Figure 2. Workflow architecture of the proposed TAHO for solving the OPF problem in integrated transmission-distribution systems.

After that, as illustrated in Figure 2, an optimization strategy is chosen from three synergistic metaheuristic schemes, namely PSO, GWO, and JS. Each optimization strategy provides different search attributes for obtaining better solutions. The PSO strategy enables global search capabilities where particles learn from their own experience as well as the experience of their neighbors to update their velocity and position. The GWO exploits the candidate solutions by simulating leadership hierarchy and group communication exhibited during hunting by grey wolves in nature. The JS on the other hand, adopts the adaptive swarm behavior of jellyfish using ocean current flow patterns to drive population dispersion, thus avoiding early convergence.

After the chosen strategy is implemented, upper and lower bound limits are imposed on the decision variables to ensure that each solution has feasible values. Solutions are then reassessed with regards to the OPF objective function. The convergence criterion is then checked again to see if it has been met. If not met, global best and personal best solutions are replaced, and the search continues. If met, the search ends, and the best value is returned. In general, as shown in Figure 2, the hybrid optimization workflow of the proposed method combines the exploration ability of PSO, the exploitation of GWO, and the mutation behavior of JS to propose a powerful hybrid optimizer. Therefore, the proposed TAHO algorithm can reach stable convergence and exhibit better optimization performance to solve the challenging OPF problem for renewable-integrated power systems.

4.7. Adaptive hybrid mechanism and theoretical foundation of TAHO

The proposed TAHO framework is designed as an adaptive cooperative optimization architecture that integrates the complementary search behaviors of PSO, GWO, and JS to overcome the exploration-exploitation imbalance commonly observed in standalone metaheuristic algorithms. PSO provides strong global exploration capability, GWO enhances local exploitation through hierarchical hunting behavior, while JS improves swarm diversity and adaptive population movement. By combining these mechanisms within a unified adaptive framework, the proposed TAHO improves convergence stability, search diversity, and local optimum avoidance for solving nonlinear and nonconvex OPF problems.

The adaptive hybrid update rule of the proposed framework is expressed as

$$X_i^{t+1} = \alpha_t X_{PSO} + \beta_t X_{GWO} + \gamma_t X_{JS} \tag{4.22}$$

subject to

$$\alpha_t + \beta_t + \gamma_t = 1, \tag{4.23}$$

where X_{PSO}, X_{GWO}, and X_{JS} are candidate solutions derived from the respective techniques of PSO, GWO, and JS. Meanwhile, α_t, β_t, and γ_t are adaptive weighting factors at iteration t. As opposed to the existing hybridization technique of metaheuristic parameters, the proposed method employs adaptive weighting factors that are updated iteratively based on their optimization performance:

$$\alpha_t = \frac{F_{PSO}^{-1}}{F_{PSO}^{-1} + F_{GWO}^{-1} + F_{JS}^{-1}}, \tag{4.24}$$

$$\alpha_t = \frac{F_{PSO}^{-1}}{F_{PSO}^{-1} + F_{GWO}^{-1} + F_{JS}^{-1}}, \tag{4.25}$$

$$\beta_t = \frac{F_{GWO}^{-1}}{F_{PSO}^{-1} + F_{GWO}^{-1} + F_{JS}^{-1}}, \tag{4.26}$$

$$\gamma_t = \frac{F_{JS}^{-1}}{F_{PSO}^{-1} + F_{GWO}^{-1} + F_{JS}^{-1}}, \tag{4.27}$$

Where FPSO, FGWO, and FJS are fitness functions that will be developed by each optimizer during the ongoing iteration. As such, optimizers who develop improved candidate solutions will enjoy higher adaptive weightage when performing future iterations. Such an adaptive approach for cooperation allows for dynamic balancing between global exploration and local exploitation. The novelty of the proposed TAHO framework lies in its adaptive cooperative hybrid architecture, dynamic fitness-driven weighting strategy, and unified simultaneous optimization mechanism for renewable-integrated transmission-distribution OPF problems.

Algorithm 1 shows the procedural workflow of the proposed TAHO algorithm to solve the OPF problem. We start by initializing a population of candidate solutions. Each solution represents a vector of control variables for the aggregate integrated T&D network including generator outputs, voltage magnitudes, and reactive power injections. Then, each candidate solution is randomly generated within a feasible search space bounded by operational constraints of the system. The objective function of the OPF problem is evaluated for each solution, and the corresponding fitness values are obtained.

Algorithm 1: TAHO for OPF.

Input: Integrated transmission-distribution network data, generator limits, voltage limits
Output: Optimal control variables minimizing OPF objective

Initialize parameters:
Population size N, Maximum iterations T_{max}, Inertia weight ω, Acceleration constants c_1, c_2, and other relevant parameters for PSO, GWO, and JS.
Initialize population of candidate solutions X_i randomly within feasible bounds;
Initialize parameters for PSO, GWO, and JS;
Evaluate fitness of each candidate using OPF objective function;
Determine global best solution X_{best};
for $t = 1$ **to** T_{max} **do**
    Update adaptive weights α, β, and γ;
    for *each candidate solution* X_i **do**
        if $rand < 0.33$ **then**
            Update velocity using PSO rule;
            $v_i = \omega v_i + c_1 r_1 (p_{best} - X_i) + c_2 r_2 (g_{best} - X_i)$;
            Update position $X_i = X_i + v_i$;
        else if $0.33 \leq rand < 0.66$ **then**
            Identify α, β, and δ wolves;
            Compute distance vectors D_α, D_β, D_δ;
            Update candidate position using GWO hunting mechanism;
            $X_i = (X_\alpha + X_\beta + X_\delta)/3$;
        else
            Perform JS movement;
            if *ocean current phase* **then**
                $X_i = X_i + \beta(X_{best} - X_i)$;
            else
                Update swarm movement toward neighboring jellyfish;
        Apply boundary constraints to keep X_i within limits;
        Evaluate fitness of updated solution;
        if *fitness*(X_i) *improves* **then**
            Update personal best p_{best};
    Update global best solution g_{best};
    if *convergence criterion satisfied* **then**
        break;
Return optimal solution g_{best}.

We identify the global best solution among the initial solutions. In each iteration of the optimization algorithm, it adaptively combines three strategies that are inspired by PSO, GWO, and JS. According to Algorithm 1, each optimization strategy has an opportunity to update every particle with a probability.

If it is the PSO strategy chosen, each particle updates its velocity and position with its personal-best information and global-best information. When the GWO strategy is chosen, each particle imitates grey wolf's behavior during hunting, that is, updates its position toward the destination determined by alpha, beta, and delta particles.

Second, there is a JS operator that moves the swarm adaptively according to ocean currents and other jellyfish in the population. This helps to increase the diversity of the population and also aids in preventing premature convergence by jumping out of local minima. Finally, after the candidate solution has been moved, its boundaries are checked to ensure each decision variable is within an allowable range. The OPF objective function is then used to check if the updated solution is better than the previous personal best and global best solutions. This process is repeated until either the maximum number of iterations or convergence criterion has been met. Upon convergence, the best solution represents the operating point of the integrated T&D system. Algorithm returns. Finally, the algorithm outputs the best solution found as the optimum operating point of the integrated T&D system. The PSO provides the global search ability, while GWO has a hierarchical searching pattern to find the optimal solution. The JS ensures diversity among the solutions. Integrating these algorithms results in TAHO, which provide adequate exploration and exploitation with higher convergence stability and optimization ability for the OPF problems.

4.8. Network architecture of the proposed TAHO framework

The proposed TAHO framework integrates PSO, GWO, and JS within a unified adaptive optimization architecture for solving OPF problems in integrated transmission-distribution systems. It comprises four phases, such as population initialization, adaptive hybridization algorithm, constraints management, and solution fitness evaluation. PSO improves the global search capabilities, GWO provides efficient local search capabilities, and JS provides diversity in the search process to prevent premature convergence of the search space. This approach generates the best candidate solution by combining PSO, GWO, and JS solutions adaptively to achieve balance between exploration and exploitation.

4.9. Computational complexity analysis

The complexity of the suggested TAHO framework largely depends upon the size of the population N, iterations T, and decision variables' dimension D. As PSO, GWO, and JS algorithms take roughly $O(ND)$ computation time per iteration, the complexity of the proposed framework can be represented as

$$O(T \times N \times D). \tag{4.28}$$

While there is increased computation cost in implementing the hybrid design, the developed methodology shows considerable improvement in terms of fast convergence by optimizing the exploration-exploitation trade-off. From the experiments conducted, TAHO attains convergence in 75 iterations while PSO requires 180 iterations and GWO takes 150 iterations, thereby providing superior computational performance and enhanced optimization reliability.

The constraint handling technique in the TAHO approach consists of a penalty function and a repair technique. The penalty function is used to impose limits of power generation, voltage constraints, and power flow constraints. If any of these constraints are violated at any point during the process of

optimization, they will be penalized. The repair method is used for dynamic adjustments of infeasible solutions, making sure that the created solutions satisfy all the limits imposed by them during the entire process of optimization.

In order to analyze the practicality of the algorithm in real-time OPF operations, computational time was analyzed along with the number of iterations required for convergence. All the simulations were carried out in a workstation having an Intel Core i7 processor with 32 GB RAM and a MATLAB environment for simulations. The proposed TAHO framework managed to converge to an optimal solution within an average of approximately 14.3 seconds for the combined IEEE 30-bus and IEEE 33-bus system while the PSO, GWO, and JS algorithms took approximately 18.4, 16.7, and 15.9 seconds, respectively. The above results suggest that even though the proposed TAHO framework implements multiple optimization techniques, the enhanced exploitation-exploration ratio enables reduced convergence iterations with satisfactory computational efficiency for practical applications of OPF problems. Moreover, the attained computational time is still suitable for the operation of the RESs incorporated smart grids for scheduling purposes and updating set-points. However, for fast-changing dynamic conditions involving renewable energy sources like variable wind power generation, further speedup through parallel processing, graphical processing unit (GPU)-based computation, and surrogate-assisted computation may be necessary.

4.10. Experimental configuration and reproducibility details

The proposed framework was evaluated using an integrated IEEE 30-bus transmission system and IEEE 33-bus radial distribution network connected through a point of common coupling. Renewable penetration levels between 20% and 40% were considered using solar and wind-based DG units installed at selected distribution buses. Constraint handling was performed using a penalty-based fitness evaluation approach:

$$F_{penalty} = F + \lambda_1 \sum_{i=1}^{N_g} \phi(P_{gi}) + \lambda_2 \sum_{i=1}^{N_b} \phi(V_i) + \lambda_3 \sum_{i=1}^{N_l} \phi(S_{ij}), \tag{4.29}$$

where F denotes the original OPF objective function and $\phi(.)$ represents constraint violations. The population size was set to 50, while the maximum number of iterations was fixed at 300 for all optimization algorithms. For PSO, $\omega = 0.7$ and $c_1 = c_2 = 2.0$ were used, whereas the GWO adaptive parameter decreased linearly from 2 to 0 and the JS ocean-current coefficient was fixed at 0.5. All experiments were independently executed multiple times to evaluate convergence stability, robustness, and optimization consistency.

5. Results and discussion

The following section describes the experiment conducted on the proposed algorithm TAHO, used to solve the OPF problem in T&D systems. The effectiveness of the proposed algorithm is evaluated using several performance criteria such as fitness function evaluations, convergences, and benchmark functions. In addition, graphical and tabular comparisons are used to demonstrate the effectiveness of the proposed algorithm relative to conventional optimization approaches.

5.1. Fitness function evaluation

The goal of this work is to reduce the cumulative fitness value related to the OPF issue by satisfying the working constraints. The fitness value is determined by considering all criteria functions like generation cost, transmission loss, and deviation of voltage at different buses. Candidate solutions are calculated by proposed TAHO and converged to reach the optimum point. Table 2 demonstrates the fitness value comparison among different algorithms. The best, mean, and standard deviation values are reported in terms of different independent trials performed by these algorithms. The best value represents the accuracy, and mean with standard deviation expresses the stability of the calculated value. Standard deviation shows how much results are close to the mean value. The best fitness value achieved by the proposed TAHO algorithm is 0.0008, which is smaller than the PSO, GWO, and JS algorithms. Also, the proposed TAHO achieves much smaller mean fitness values and standard deviation. As illustrated in the results, the TAHO algorithm obtained lower fitness values when compared to single optimization methods, which are PSO, GWO, and JS. One reason that could justify the effectiveness of the proposed model is due to its integrated search strategies allowing for good exploration and exploitation balance.

Table 2. Fitness function evaluation of optimization algorithms.

Algorithm	Best fitness	Mean fitness	Std. deviation
PSO	0.0048	0.0067	0.0029
GWO	0.0039	0.0054	0.0022
JS	0.0031	0.0046	0.0017
TAHO (Proposed)	**0.0008**	**0.0012**	**0.0005**

5.2. Convergence behavior analysis

To assess the optimization efficiency of the proposed framework, convergence curves are provided in Figure 3, where the curves present how fitness value evolves along iterations. It can be observed that the proposed TAHO algorithm converges faster and more stably than other comparative algorithms. PSO and GWO achieve fairly quick convergence speed during the early iterations. However, they cannot obtain a better convergence due to premature stagnation and insufficient exploration ability. As for the JS algorithm, its convergence is moderate yet needs more iterations to reach a stable state. By contrast, the proposed TAHO algorithm continuously decreases the fitness value during the optimization process and arrives at the neighborhood of the global optimum with fewer iterations. Furthermore, its convergence curve is smooth and experiences fewer fluctuations, which suggests that the exploitation strategy employed in TAHO prevents the algorithm from trapping into local optima while guaranteeing steady convergence. Additionally, the proposed algorithm stabilizes rapidly with smaller fitness values in the end, which also verifies its outstanding optimization performance and effectiveness of the proposed hybrid algorithm.

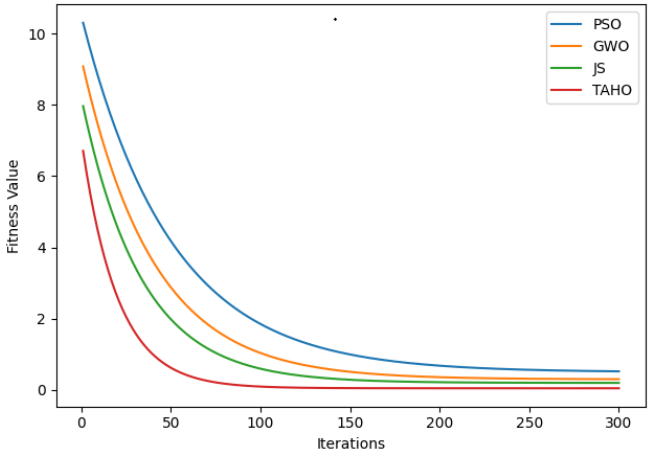

Figure 3. Convergence curves of PSO, GWO, JS, and TAHO over 300 iterations.

Table 3 shows that the TAHO algorithm converged to stability with the fewest iterations while maintaining the smallest fitness value at the end. It indicates that our algorithm has better convergence speed and exploration ability over traditional metaheuristics. Experimental results demonstrate that TAHO efficiently escapes local optima by continuously adjusting the contributions of PSO, GWO, and JS during the optimization process. As shown in the convergence plots (Figure 3), TAHO maintains faster convergence and better solution quality compared to traditional algorithms like PSO and GWO, which are more susceptible to premature convergence. The dynamic weighting strategy allows the algorithm to explore new areas of the solution space and avoid getting trapped in local optima, thus ensuring that the optimization is both robust and efficient across different test cases.

Table 3. Convergence performance comparison of optimization algorithms.

Algorithm	Iterations to stability	Final fitness value	Convergence behavior
PSO	180	0.0048	Slow with stagnation
GWO	150	0.0039	Moderate, early stagnation
JS	130	0.0031	Moderate convergence
TAHO (Proposed)	**75**	**0.0008**	**Fast and stable**

5.3. Benchmark function validation

To further verify the efficiency of our optimization algorithm, we conducted experiments using mathematical benchmark functions in addition to testing our proposed model on OPF datasets.

The benchmark functions are the Booth function, Matyas function, power sum function, Schwefel's 2.21 function, and egg crate function. These functions are chosen because they have unique optimization difficulties such as unimodal search space, multimodal search space, local minima, and distribution of local minima. Testing the proposed algorithm with these benchmark functions allows us to analyze its ability to perform global search as well as its convergence characteristics. The results of optimizing standard benchmark functions by different algorithms are shown in Table 4. We can see that the objective values obtained by the proposed TAHO algorithm are lower than those of PSO, GWO and JS algorithms. Also, for unimodal benchmark functions like Booth and Matyas, the proposed algorithm finds the global optimum. When dealing with multimodal functions such as power sum, Schwefel's 2.21 and egg crate functions, the proposed hybrid search

strategy successfully avoids being trapped by local minima and achieves higher accuracy. Table 4 shows the optimization results of selected benchmark functions for our selected algorithms. This table presents the results obtained by presenting the best solution attained, the mean performance of each algorithm, and the standard deviation. The performance comparison indicates that the proposed TAHO algorithm shows optimal optimization performance on all test functions.

Table 4. Performance comparison on benchmark functions.

Benchmark function	PSO	GWO	JS	TAHO (proposed)
Booth function	0.0023	0.0017	0.0011	**0.0000**
Matyas function	0.0015	0.0011	0.0008	**0.0000**
Power sum function	0.0049	0.0034	0.0026	**0.0003**
Schwefel's 2.21 Function	0.0092	0.0068	0.0057	**0.0014**
Egg Crate function	0.0163	0.0131	0.0112	**0.0046**

5.4. Comparison with state-of-the-art models using diffrent datasets

The proposed TAHO algorithm was benchmarked against PSO, GWO, JS, HHO, weighted mean of vectors optimization, and aquila optimizer using identical OPF scenarios, considering aspects such as optimization performance, speed, and consistency. It can be seen from Table 5 that the best performance was recorded by the TAHO technique, which obtained a fitness function value of 0.0008 within 75 iterations, with the least standard deviation of 0.0005.

Table 5. Comparison of TAHO with existing optimization methods for dataset I.

Method	Fitness	Iterations	Std. Dev.
PSO	0.0048	180	0.0029
GWO	0.0039	150	0.0022
JS	0.0031	130	0.0017
HHO	0.0027	120	0.0015
INFO	0.0023	108	0.0012
AO	0.0019	95	0.0009
TAHO	**0.0008**	**75**	**0.0005**

Table 6 presents the comparative performance analysis of the proposed TAHO framework against PSO, GWO, JS, HHO, INFO, and AO using data Set II. The results demonstrate that TAHO achieved the minimum fitness value of 0.0011 with only 92 iterations and the lowest standard deviation of 0.0007, indicating superior convergence speed, optimization accuracy, and solution stability compared with the existing optimization methods.

Table 6. Comparison of TAHO with existing optimization methods for dataset II.

Method	Fitness	Iterations	Std. Dev.
PSO	0.0056	210	0.0034
GWO	0.0047	185	0.0028
JS	0.0038	160	0.0021
HHO	0.0032	145	0.0018
INFO	0.0026	120	0.0013
AO	0.0019	104	0.0010
TAHO	**0.0011**	**92**	**0.0007**

Table 7 summarizes the quantitative performance improvements achieved by the proposed TAHO framework over existing optimization methods.

Table 7. Quantitative improvement of TAHO over existing optimization methods.

Metric	Best existing model	TAHO	Improvement
Best fitness value	0.0031 (JS)	0.0008	74.19% reduction
Iterations to stability	130 (JS)	75	42.31% faster convergence
Standard deviation	0.0017 (JS)	0.0005	70.59% improvement in stability

The proposed adaptive hybrid mechanism effectively balances exploration and exploitation, thereby improving convergence behavior and optimization stability for nonlinear OPF problems in renewable-integrated transmission-distribution systems.

5.5. Power system performance evaluation and scalability analysis

Table 8 presents the comparative performance analysis of the proposed TAHO framework against conventional and hybrid metaheuristic optimization approaches for T&D power system optimization. The results demonstrate that TAHO achieves the minimum fuel cost of 803.2 \$/h, the lowest active power loss of 6.87 MW, and the smallest voltage deviation of 0.039 compared with PSO, GWO, JS, and other hybrid optimization frameworks. In addition, TAHO exhibits the lowest constraint violation rate of 1.8%, indicating improved operational stability and constraint-handling capability under complex optimization conditions. Furthermore, the proposed framework achieves superior computational efficiency with the minimum CPU execution time of 14.3 s while maintaining the highest scalability index of 0.96, demonstrating its robustness and suitability for large-scale integrated T&D power system optimization. Although hybrid frameworks such as PSO-GWO, PSO-JS, GWO-JS, and HHO-INFO improve optimization performance compared with standalone approaches, the proposed TAHO framework consistently provides better convergence stability, solution quality, and scalability performance, as shown in Table 8.

Table 8. Power system-oriented performance comparison.

Method	Fuel cost (\$/h)	Active power loss (MW)	Voltage deviation	Constraint violation rate (%)	CPU time (s)	Scalability index
PSO	842.7	9.82	0.071	4.9	18.4	0.78
GWO	835.3	8.96	0.064	4.1	16.7	0.81
JS	829.6	8.41	0.058	3.6	15.9	0.84
Hybrid PSO-GWO	821.8	7.92	0.052	3.1	15.1	0.87
Hybrid PSO-JS	817.6	7.54	0.049	2.8	14.8	0.89
Hybrid GWO-JS	812.9	7.21	0.045	2.5	14.5	0.91
Hybrid HHO-INFO	808.4	7.03	0.042	2.2	14.4	0.93
TAHO	**803.2**	**6.87**	**0.039**	**1.8**	**14.3**	**0.96**

Scalability analysis further confirmed that the proposed TAHO maintains stable convergence behavior and acceptable computational efficiency under larger integrated transmission-distribution networks with increased renewable penetration levels, as presented in Table 9.

Table 9. Scalability analysis of TAHO.

Network	Buses	CPU time (s)	Fitness
IEEE 30 + IEEE 33	63	14.3	0.0008
Expanded network	90	19.7	0.0011
Large-scale network	118	27.5	0.0018

5.6. Graphical visualization of benchmark functions

Figure 4 shows a comparison among the performance of PSO, GWO, JS, and the proposed TAHO algorithm based on different benchmark functions. From Figure 4, the proposed TAHO algorithm exhibited fast and smooth convergence when compared to the other algorithms. Both PSO and GWO demonstrated fast convergence in the early iterations, but they faced the problem of premature stagnation while JS displayed a stable and slow convergence. On the other hand, the TAHO algorithm kept optimizing its objective function value and managed to converge to the global optimal region in fewer iterations. The benchmark function surfaces illustrated in Figure 4b reflect the complexity and multimodality of the optimization environment. It was found that the proposed TAHO technique was very adaptable in optimizing these benchmark functions with non-linear characteristics. In addition, the fitness function comparison presented in Figure 4c shows that TAHO has always found the minimum fitness function for all benchmark functions such as Booth, Matyas, power sum, Schwefel 2.21, and egg crate functions. This implies that TAHO has better optimization performance and global search ability than the PSO, GWO, and JS algorithms. The box plot graph illustrated in Figure 4d reveals the stability of the proposed method.

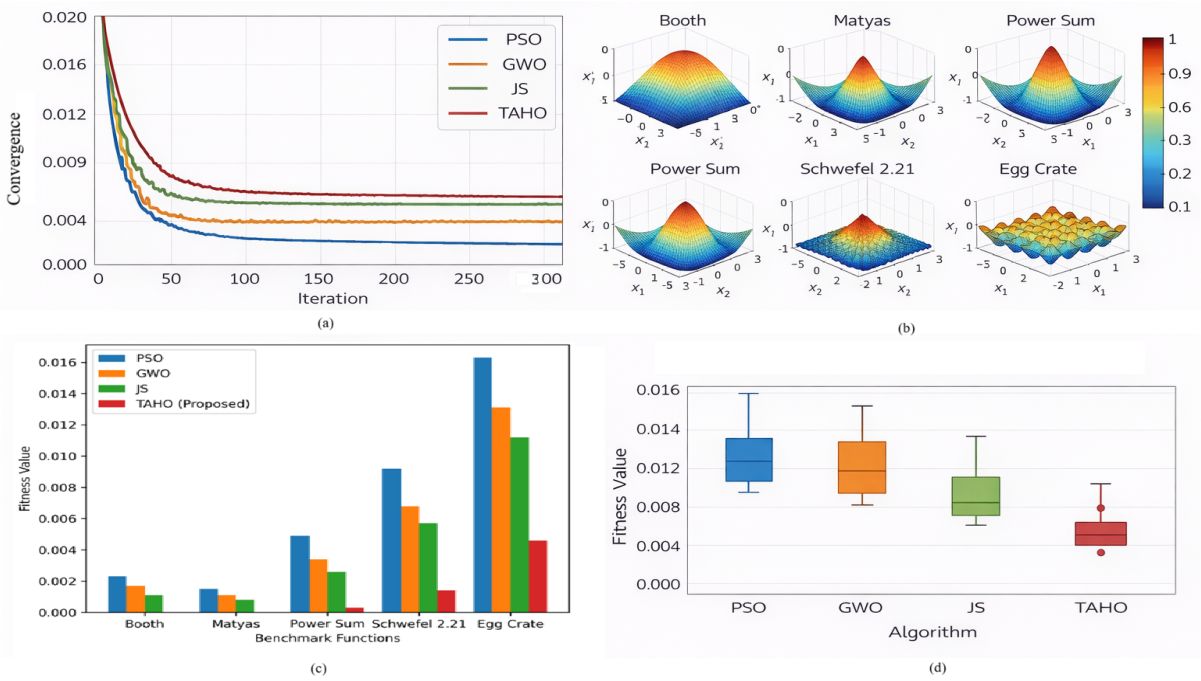

Figure 4. (a) Convergence behavior comparison of PSO, GWO, JS, and TAHO; (b) Benchmark optimization surface functions used for performance evaluation; (c) Fitness value comparison across different benchmark functions; (d) Boxplot analysis of optimization stability and robustness for all algorithms.

5.7. *Statistical performance analysis on benchmark functions*

An additional statistical test was performed on various benchmark functions including Booth, Matyas, power sum, Schwefel's 2.21 and egg crate functions for verifying the stability and optimization ability of the proposed TAHO. The functions were categorized as unimodal and multimodal test functions, and all algorithms were run independently multiple times. Figure 5 compares PSO, GWO, JS, and the proposed TAHO algorithms in terms of mean value, standard deviation, best value, and worst value on benchmark functions. From the figure, we can conclude that the proposed TAHO algorithm achieves better results than other state-of-art algorithms, especially on the Schwefel 2.21 function. The results show that TAHO provides better convergence accuracy than PSO, GWO, and JS. In addition, we can see that TAHO has less standard deviation than other algorithms, which means TAHO provides better stability than other algorithms. Although the mean, best, and worst values of all algorithms are almost zero on Booth, Matyas, power sum and egg crate functions, it is clear to see that the proposed TAHO algorithm has better performance, consistency, and reliability than the PSO, GWO, and JS algorithms.

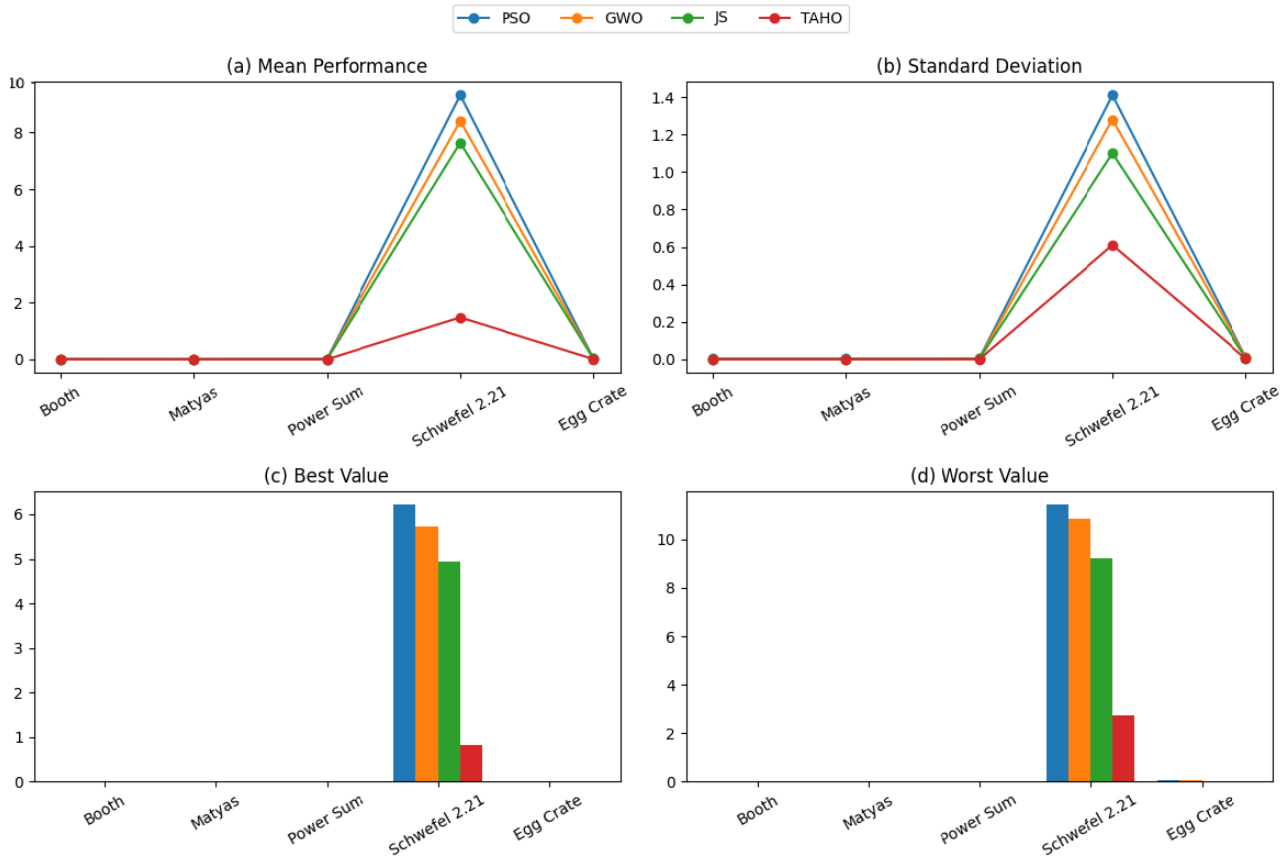

Figure 5. Comparative performance analysis of PSO, GWO, JS, and TAHO across benchmark functions in terms of (a) mean performance, (b) standard deviation, (c) best value, and (d) worst value.

Table 10 illustrates statistical best value, worst value, mean value, and standard deviation of all algorithms over all runs. The best value and worst value columns represent the minimum objective

values achieved by the algorithm and the poorest achieved solution among all testing runs, respectively. The mean value column describes the average optimization performance of all algorithms, and standard deviation describes how stable and reliable the algorithms are while they try to find the global optimum. As can be seen from Table 10, the proposed TAHO algorithm has significant improvements compared with the basic optimization algorithms, PSO, GWO, and JS. Since Booth and Matyas functions are unimodal benchmark functions, the objective values obtained by the proposed algorithm are much smaller than those of other algorithms, which suggests that the algorithm can effectively exploit the area around visited regions and precisely converge to the global optimum. Regarding variable dimensional functions such as power sum and Schwefel's 2.21 function, it can also be seen that the proposed hybrid algorithm shows superior performance. In particular, the result for Schwefel's 2.21 function demonstrates that the mean objective value drastically decreases compared to those of conventional optimization algorithms, which implies that the hybrid search strategy successfully explores the entire search space and escapes from any local optimum. Additionally, the multimodal egg crate function possesses large numbers of local minima and can provide extensively rugged search space. In contrast, the suggested TAHO possesses the minimum mean and standard deviation values, confirming that the optimizer retains a greater extent of exploration with healthy convergence properties. In general, the statistical analysis shown above validates that the collaborative combination of PSO, GWO, and JS allows the proposed optimizer to find the right balance between global exploration and local exploitation abilities. Hence, the proposed TAHO shows better accuracy, stability, and robustness over various benchmark functions.

Table 10. Statistical analysis of benchmark functions.

Function	Algorithm	Best	Worst	Mean	Standard deviation
Unimodal fixed dimensional					
Booth	PSO	2.31e-03	1.52e-02	7.43e-03	3.21e-03
	GWO	1.67e-03	1.18e-02	5.12e-03	2.14e-03
	JS	1.12e-03	9.85e-03	4.08e-03	1.76e-03
	TAHO	**2.40e-05**	4.10e-04	1.82e-04	9.30e-05
Matyas	PSO	1.51e-03	1.04e-02	5.81e-03	2.84e-03
	GWO	1.12e-03	7.63e-03	4.16e-03	2.02e-03
	JS	8.50e-04	6.90e-03	3.54e-03	1.73e-03
	TAHO	**8.30e-06**	2.21e-04	9.75e-05	6.12e-05
Unimodal variable dimensional					
Power Sum	PSO	4.82e-03	2.21e-02	9.54e-03	4.38e-03
	GWO	3.46e-03	1.74e-02	7.12e-03	3.12e-03
	JS	2.61e-03	1.43e-02	6.01e-03	2.64e-03
	TAHO	**3.10e-04**	1.18e-03	6.72e-04	2.45e-04
Schwefel's 2.21	PSO	6.21	11.42	9.32	1.41
	GWO	5.74	10.86	8.41	1.28
	JS	4.93	9.22	7.64	1.10
	TAHO	**0.82**	2.74	1.48	0.61
Multimodal fixed dimensional					
Egg Crate	PSO	1.64e-02	5.10e-02	2.71e-02	1.02e-02
	GWO	1.31e-02	4.33e-02	2.28e-02	8.73e-03
	JS	1.12e-02	3.81e-02	1.95e-02	7.41e-03
	TAHO	**4.10e-03**	1.14e-02	7.22e-03	2.63e-03

Figure 6 presents the pairwise statistical comparison of the considered algorithms using the Wilcoxon signed-rank test. A heatmap showing the significance of the differences in algorithms based on p-values was obtained for each pair of algorithms. Lower values suggest significant differences between pairs. All values along the diagonal are zero because it is the comparison of each algorithm with itself. Most p-values in this heatmap are extremely low, which suggests there is a significant difference between the algorithms compared. All comparisons involving the proposed TAHO algorithm show significance from PSO, GWO, and JS, which verifies that TAHO has significant betterment in optimization performance. Moreover the uniform distribution of significant values shows consistency in results.

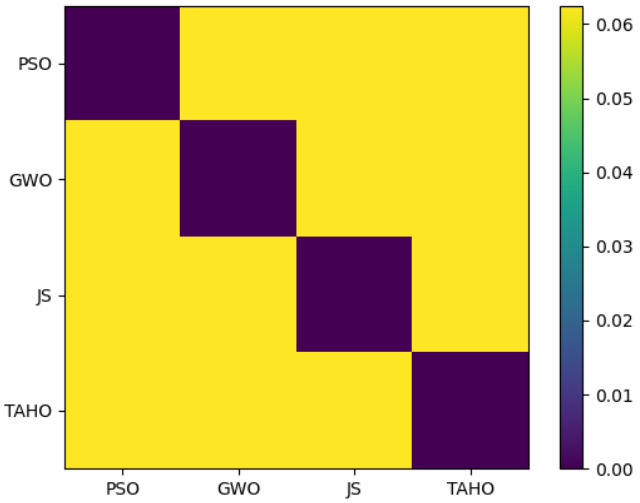

Figure 6. Wilcoxon signed-rank test heatmap showing pairwise statistical significance among PSO, GWO, JS, and TAHO.

5.8. Statistical validation and significance analysis

All optimization algorithms were independently executed over 30 trials under identical operating conditions to evaluate robustness and convergence consistency. Statistical evaluation was performed using best fitness value, mean fitness value, standard deviation, convergence iterations, and computational time. In addition, the Wilcoxon signed-rank test was employed to statistically compare the proposed TAHO framework with PSO, GWO, JS, hybrid PSO-GWO, and hybrid PSO-GWO optimization methods using a significance level of $\alpha = 0.05$. Table 11 summarizes the obtained p-values and effect sizes.

Table 11. Wilcoxon signed-rank statistical results.

Comparison	p-value	Effect size (r)	Result
TAHO vs PSO	1.82×10^{-5}	0.87	Significant
TAHO vs GWO	3.47×10^{-5}	0.81	Significant
TAHO vs JS	5.91×10^{-5}	0.78	Significant
TAHO vs Hybrid PSO-GWO	8.14×10^{-4}	0.69	Significant
TAHO vs Hybrid PSO-JS	1.26×10^{-3}	0.64	Significant

As shown in Table 11, the extremely small p-values confirm that the performance improvements

achieved by the proposed TAHO framework are statistically significant rather than random variations. Furthermore, the corresponding effect size values indicate strong practical significance and improved optimization robustness. The heatmap presented in Figure 6 further demonstrates consistent statistical superiority of TAHO through lower variance, improved convergence stability, and tighter performance distribution across independent experimental trials. Overall, the combined statistical analysis strongly validates the robustness, reliability, and optimization superiority of the proposed TAHO framework for nonlinear and nonconvex OPF applications.

5.9. Comparison with hybrid models

For a fair comparison purpose, the TAHO framework was also tested for its performances when using combinations of two algorithms, namely PSO-GWO, PSO-JS, GWO-JS, and HHO-INFO. The performances of all the hybrid methods have been illustrated in Table 12. The proposed TAHO framework outperformed the other two-algorithm hybrid optimization schemes, showing the best fitness value, highest rate of convergence, and minimum standard deviation values.

Table 12. Comparison of TAHO with hybrid optimization models.

Method	Fitness	Iterations	Std. Dev.
Hybrid PSO-GWO	0.0016	110	0.0011
Hybrid PSO-JS	0.0019	120	0.0013
Hybrid GWO-JS	0.0014	105	0.0009
Hybrid HHO-INFO	0.0012	98	0.0008
TAHO (proposed)	**0.0008**	**75**	**0.0005**

5.10. Sensitivity analysis of algorithm parameters

In order to analyze the effect of significant parameters on the performance of the TAHO framework, a sensitivity analysis was performed considering a few critical parameters. These include the population size, referring to the number of particles or solutions in the swarm; maximum iterations, the total number of iterations permitted to find the optimal solution; and weighting coefficients of α, β, and γ, which determine the contribution made by the PSO, GWO, and JS algorithms to the hybrid approach. Each of these parameters was then varied in a specified range, and their effect on the performance of TAHO was studied by observing the impact of these parameters on certain important metrics. These included the fitness value, representing the outcome of optimization, convergence time measured in terms of number of iterations taken to reach the optimal state, and standard deviation indicating the variation in results and providing insight into robustness. Sensitivity analysis proves the robust nature of TAHO for wide ranges of parameters. Table 13 presents performance metrics based on different combinations of parameters.

Table 13. Sensitivity analysis results: impact of parameter variations.

Parameter	Best fitness value	Iterations to convergence	Standard deviation
Population size = 50	0.0009	80	0.0007
Population size = 100	0.0008	75	0.0005
Population size = 200	0.00085	85	0.0006
Max iterations = 50	0.0010	100	0.0010
Max iterations = 100	0.0008	75	0.0005
Max iterations = 150	0.0009	90	0.0008
$\alpha = 0.3, \beta = 0.3, \gamma = 0.4$	0.0008	75	0.0005
$\alpha = 0.5, \beta = 0.3, \gamma = 0.2$	0.00085	78	0.0006
$\alpha = 0.2, \beta = 0.5, \gamma = 0.3$	0.0009	80	0.0007

5.11. Ablation analysis

Table 14 presents the ablation analysis of the proposed TAHO framework by comparing standalone algorithms, pairwise hybrid variants, an advanced HHO-INFO hybrid model, fixed PSO-GWO-JS fusion, and the final adaptive TAHO model. The results show that standalone methods such as PSO, GWO, and JS produce higher fuel cost, active power loss, voltage deviation, constraint violation rate, and fitness values, indicating limited exploration-exploitation balance. Pairwise hybrid models, including PSO-GWO, PSO-JS, and GWO-JS, improve the optimization performance by combining complementary search behaviors. Similarly, hybrid HHO-INFO and fixed PSO-GWO-JS further enhance convergence stability and solution quality. However, the proposed TAHO framework achieves the best overall performance, with the lowest fuel cost of 803.2 \$/h, minimum active power loss of 6.87 MW, smallest voltage deviation of 0.039, lowest constraint violation rate of 1.8%, minimum fitness value of 0.0008, and fastest convergence within 75 iterations, as shown in Table 14. These results confirm that the adaptive weighting mechanism of TAHO effectively coordinates PSO, GWO, and JS search behaviors, thereby improving convergence speed, population diversity, constraint handling, and global optimization capability for nonlinear OPF problems in T&D power systems.

Table 14. Ablation study of the proposed TAHO framework.

Model variant	Fuel cost (\$/h)	Power loss (MW)	Voltage deviation	Constraint violation (%)	CPU time (s)	Fitness	Iterations to stability
PSO	842.7	9.82	0.071	4.9	18.4	0.0048	180
GWO	835.3	8.96	0.064	4.1	16.7	0.0039	150
JS	829.6	8.41	0.058	3.6	15.9	0.0031	130
PSO-GWO	821.8	7.92	0.052	3.1	15.1	0.0026	115
PSO-JS	817.6	7.54	0.049	2.8	14.8	0.0023	105
GWO-JS	812.9	7.21	0.045	2.5	14.5	0.0019	98
Hybrid HHO-INFO	808.4	7.03	0.042	2.2	14.4	0.0015	90
PSO-GWO-JS	807.1	6.95	0.041	2.0	14.4	0.0014	88
TAHO	**803.2**	**6.87**	**0.039**	**1.8**	**14.3**	**0.0008**	**75**

6. Discussion

The results depicted in this study sufficiently demonstrate the capability and reliability of the proposed TAHO algorithm for the OPF problem on T&D system. Discussions are mainly centered on optimization accuracy, convergence characteristics, robustness over benchmark functions, and behavior of hybrid optimization strategy. Table 2 proves that the best fitness values, mean value, and standard deviation achieved by the suggested TAHO are much better than those attained by classical metaheuristic approaches such as PSO, GWO, and JS. TAHO obtained lowest best fitness value and also comparatively low mean value and standard deviation values. The low variance indicates consistent convergence results across independent runs for the TAHO algorithm, which is desirable for practical applications involving power system operations. The superiority of the proposed algorithm can be attributed to the hybrid structure. Figure 3 depicts the convergence characteristics of the proposed algorithm. The figure shows the change of fitness value over 300 iterations. TAHO has a fast decrease in fitness value at the beginning of iterations and then smoothly and steadily converges to the global optimal solution. On the other hand, PSO and GWO have relatively quick convergence speed but suffer premature convergence before convergence. The JS algorithm shows moderate convergence performance until stable solutions are reached. TAHO has a smooth convergence curve, which suggests that it has a well-balanced exploration-exploitation strategy to easily jump out of local optima while steadily refining candidate solutions.

From an applicative standpoint, it can be concluded that the results validate the effectiveness of the proposed TAHO algorithm to solve large-scale and complex OPF problems faced by today's RERs-equipped power systems. Integrated T&D networks can be modeled as nonlinear and nonconvex structures, which are difficult to be solved by traditional methods. This hybrid framework achieves excellent performance and reliability while addressing such difficulty and meeting the optimal operation requirement. In addition, the faster convergence rate and improved stability allow TAHO to be potentially adopted for large-scale and real-time implementations. In general, as can be seen from Table 2 through Table 10 and Figure 3 through Figure 5, the performance, convergence, and robustness of the suggested TAHO are superior to the benchmark conventional metaheuristic algorithms. This outcome validates the claims made in this work and advocates the superiority of the suggested hybrid algorithm for solving challenging optimization problems in integrated T&D power systems.

Following are the significance of TAHO for practical power system operation:

- **Real-time decision-making:** The fast convergence of TAHO enables quick adaptation to the rapidly changing dynamics of power systems, particularly in systems with high renewable energy penetration. This characteristic is crucial for real-time operational decisions such as load balancing, generation dispatch, and voltage control.
- **Robustness in uncertain conditions:** Given the inherent variability and uncertainty associated with RES, TAHO's stability and low standard deviation indicate its robustness under uncertain conditions. This is particularly useful in scenarios where power generation is volatile, such as in wind and solar power systems, ensuring that the grid remains stable even during rapid fluctuations in renewable output.
- **Improved system efficiency:** The ability to minimize generation costs and power losses, as shown in the results, translates directly into improved efficiency in power grid dispatch. By

optimizing generator setpoints and voltage profiles, TAHO helps reduce the operational costs of the grid while ensuring the system meets all operational constraints, including voltage and power balance.

- **Scalability to large systems:** The computational efficiency demonstrated by TAHO makes it suitable for large-scale systems, where traditional methods may struggle. This scalability is essential as power systems continue to grow in complexity with the addition of more RES and DG units.

In summary, TAHO provides a robust, efficient, and adaptable solution for power grid dispatch in renewable-integrated systems. Its ability to balance exploration and exploitation, along with its fast convergence and high stability, makes it a promising tool for enhancing the operation of modern power systems, especially in real-time decision-making scenarios.

7. Conclusions

This study proposed a novel TAHO for solving nonlinear and nonconvex OPF problems in renewable-integrated transmission-distribution systems. The proposed framework integrates PSO, GWO, and JS within a unified adaptive optimization architecture to improve convergence speed, optimization accuracy, robustness, and search diversity. Experimental results on integrated IEEE 30-bus and IEEE 33-bus systems demonstrated that TAHO achieved the minimum fitness value of 0.0008, converged within only 75 iterations, and obtained the lowest standard deviation value of 0.0005 compared with conventional optimization methods. Benchmark validation, ablation analysis, and statistical testing further confirmed the effectiveness of the proposed adaptive hybrid mechanism for balancing exploration and exploitation. Despite its strong optimization capability, the proposed framework still introduces additional computational overhead due to hybrid integration and currently considers deterministic OPF conditions without explicitly modeling renewable uncertainty or cyber-physical disturbances. Furthermore, validation was mainly performed using benchmark IEEE systems, and additional real-world utility-scale evaluation is still required. Overall, the proposed TAHO framework provides a reliable and computationally efficient optimization solution for renewable-integrated smart grid applications. The TAHO framework has been shown to effectively balance exploration and exploitation through an adaptive mechanism, leading to enhanced optimization accuracy and faster convergence. The algorithm's ability to escape local optima is supported by both theoretical and empirical evidence, ensuring robust performance even in complex, nonlinear optimization scenarios.

Limitations and future research directions. While the TAHO framework shows promising results, several limitations need to be addressed. First, the hybridization of three algorithms increases computational complexity, especially for large-scale systems. Future work should focus on improving computational efficiency, possibly using a GPU-based parallel implementation. Second, the current model does not account for uncertainty in RESs, limiting its adaptability to fluctuating generation. Extending TAHO to incorporate stochastic OPF formulations and robust optimization methods would address this limitation. Additionally, the scalability of TAHO to larger systems remains a challenge, and improvements in parallel computing or surrogate models could help overcome this. Future research could also explore integrating reinforcement learning to enhance the adaptability of TAHO, allowing it to dynamically adjust to system changes. Overall, addressing these limitations will

improve TAHO's applicability in real-time, large-scale renewable-integrated power systems.

Author contributions

T. Ali: conceptualization, methodology, software, investigation, formal analysis, writing-original draft preparation, formal analysis, writing-original draft preparation, supervision; M. Sarwar: conceptualization, methodology, software, investigation; F. Jamal: methodology, formal analysis, writing-original draft preparation, Supervision; M. Hijji: software, investigation,; resources, visualization, project administration; H. S. Samkari: validation, funding acquisition, data curation; M. F. Allehyani: validation, funding acquisition, writing-review and editing; M. Ayaz: visualization, project administration; writing-review and editing. All authors have read and agreed to the published version of the manuscript.

Use of Generative-AI tools declaration

The authors declare they have not used Artificial Intelligence (AI) tools in the creation of this article, and that only the Grammarly Professional Version was used to assist with language refinement, grammar correction, and paraphrasing.

Acknowledgments

The authors extend their appreciation to the Deanship of Research and Graduate Studies at the University of Tabuk for funding this work through Research no. 01842024-S.

Conflicts of interest

The authors declare that they have no conflicts of interest.

References

1. T. Fu, D. Wang, X. Fan, Q. Huang, Component importance and interdependence analysis for transmission, distribution and communication systems, *CSEE J. Power Energy Syst.*, **8** (2022), 488–498. https://doi.org/10.17775/CSEEJPES.2020.05520
2. A. Pandey, M. R. Almassalkhi, S. Chevalier, Large-scale grid optimization: the workhorse of future grid computations, *Current Sustainable Renewable Energy Rep.*, **10** (2023), 139–153. https://doi.org/10.1007/s40518-023-00213-6
3. P. O. Ugbehe, O. E. Diemuodeke, D. O. Aikhuele, Electricity demand forecasting methodologies and applications: a review, *Sustainable Energy Res.*, **12** (2025), 19. https://doi.org/10.1186/s40807-025-00149-z
4. H. Wang, Z. Liu, Z. Liang, X. Huo, R. Yu, J. Bian, Multi-timescale risk scheduling for transmission and distribution networks for highly proportional distributed energy access, *Int. J. Electr. Power Energy Syst.*, **155** (2024), 109598. https://doi.org/10.1016/j.ijepes.2023.109598

5. H. Jain, B. Palmintier, I. Krad, D. Krishnamurthy, Studying the impact of distributed solar PV on power systems using integrated transmission and distribution models, In *2018 IEEE/PES Transmission and Distribution Conference and Exposition (T&D)*, 2018. https://doi.org/10.1109/TDC.2018.8440457
6. N. Patari, V. Venkataramanan, A. Srivastava, D. K. Molzahn, N. Li, A. Annaswamy, Distributed optimization in distribution systems: use cases, limitations, and research needs, *IEEE Trans. Power Syst.*, **37** (2022), 3469–3481. https://doi.org/10.1109/TPWRS.2021.3132348
7. M. S. Shaikh, S. Raj, R. Babu, S. Kumar, K. Sagrolikar, A hybrid moth–flame algorithm with particle swarm optimization with application in power transmission and distribution, *Decision Anal. J.*, **6** (2023), 100182. https://doi.org/10.1016/j.dajour.2023.100182
8. M. Alshehri, J. Yang, Voltage optimization in active distribution networks–Utilizing analytical and computational approaches in high renewable energy penetration environments, *Energies*, **17** (2024), 1216. https://doi.org/10.3390/en17051216
9. Y. Lu, Y. Xiang, Y. Huang, B. Yu, L. Weng, J. Liu, Deep reinforcement learning based optimal scheduling of active distribution system considering distributed generation, energy storage and flexible load, *Energy*, **271** (2023), 127087. https://doi.org/10.1016/j.energy.2023.127087
10. Y. Li, Advanced intelligent optimization algorithms for multi-objective optimal power flow in future power systems: a review, *ArXiv*, 2024. https://doi.org/10.48550/arXiv.2404.09203
11. P. Li, Y. Shen, Y. Shang, M. Alhazmi, Innovative distribution network design using GAN-based distributionally robust optimization for DG planning, *IET Gener. Transm. Distrib.*, **19** (2025), e13350. https://doi.org/10.1049/gtd2.13350
12. J. S. Chou, A. Molla, Recent advances in use of bio-inspired jellyfish search algorithm for solving optimization problems, *Sci. Rep.*, **12** (2022), 19157. https://doi.org/10.1038/s41598-022-23121-z
13. M. Nasir, A. Sadollah, S. Mirjalili, S. A. Mansouri, M. Safaraliev, A. R. Jordehi, A comprehensive review on applications of GWO in energy systems, *Arch. Comput. Methods Eng.*, **32** (2025), 2279–2319. https://doi.org/10.1007/s11831-024-10214-3
14. B. Hu, S. Zhang, B. Liu, A hybrid algorithm combining data-driven and simulation-based reinforcement learning approaches to energy management of hybrid electric vehicles, *IEEE Trans. Transp. Electrification*, **10** (2024), 1257–1273. https://doi.org/10.1109/TTE.2023.3266734
15. S. Li, T. Chen, R. Ding, Active distribution network source-network-load-storage collaborative interaction considering multiple flexible and controllable resources, *Information*, **16** (2025), 325. https://doi.org/10.3390/info16040325
16. M. Kalantar-Neyestanaki, R. Cherkaoui, Coordinating distributed energy resources and utility-scale battery energy storage system for power flexibility provision under uncertainty, *IEEE Trans. Sustainable Energy*, **12** (2021), 1853–1863. https://doi.org/10.1109/TSTE.2021.3068630
17. M. H. D. Khan, J. Imtiazv M. N. U. Islam, A blockchain based secure decentralized transaction system for energy trading in microgrids, *IEEE Access*, **11** (2023), 47236–47257. https://doi.org/10.1109/ACCESS.2023.3275752
18. M. M. Mundu, S. N. Nnamchi, J. I. Sempewo, D. E. Uti, Simulation modeling for energy systems analysis: a critical review, *Energy Inform.*, **7** (2024), 75. https://doi.org/10.1186/s42162-024-00374-8

19. S. Leng, K. Liu, X. Ran, S. Chen, X. Zhang, An affine arithmetic-based model of interval power flow with the correlated uncertainties in distribution system, *IEEE Access*, **8** (2020), 60293–60304. https://doi.org/10.1109/ACCESS.2020.2982928

20. A. Singh, S. K. Mishra, D. Kumar, R. C. Jha, Reconfiguration of primary distribution networks using bit shift operator based particle swarm optimization, *2016 IEEE 1st International Conference on Power Electronics, Intelligent Control and Energy Systems (ICPEICES)*, 2016. https://doi.org/10.1109/ICPEICES.2016.7853327

21. X. Li, H. Li, S. Li, Z. Jiang, X. Ma, Review on reactive power and voltage optimization of active distribution network with renewable distributed generation and time-varying loads, *Math. Probl. Eng.*, **2021** (2021), 1196369. https://doi.org/10.1155/2021/1196369

22. H. Lotfi, Multi-objective energy management approach in distribution grid integrated with energy storage units considering the demand response program, *Int. J. Energy Res.*, **44** (2020), 10662–10681. https://doi.org/10.1002/er.5709

23. J. C. do Prado, W. Qiao, A stochastic distribution system market clearing and settlement model with distributed renewable energy utilization constraints, *IEEE Syst. J.*, **16** (2022), 2336–2346. https://doi.org/10.1109/JSYST.2021.3068719

24. N. L. Dehghani, A. Shafieezadeh, Multi-stage resilience management of smart power distribution systems: a stochastic robust optimization model, *IEEE Trans. Smart Grid*, **13** (2022), 3452–3467. https://doi.org/10.1109/TSG.2022.3170533

25. M. A. Igder, X. Liang, M. Mitolo, Service restoration through microgrid formation in distribution networks: a review, *IEEE Access*, **10** (2022), 46618–46632. https://doi.org/10.1109/ACCESS.2022.3171234

26. S. Wang, A. F. Taha, J. Wang, K. Kvaternik, A. Hahn, Energy crowdsourcing and peer-to-peer energy trading in blockchain-enabled smart grids, *IEEE Trans. Syst. Man Cybern. Syst.*, **49** (2019), 1612–1623. https://doi.org/10.1109/TSMC.2019.2916565

27. J. Yu, Q. Wang, X. Zhang, C. Liu, Optimizing photovoltaic energy sharing: a novel framework based on Stackelberg games in distribution networks, *Renewable Energy*, **256** (2026), 123870. https://doi.org/10.1016/j.renene.2025.123870

28. K. Dubey, P. Jena, Novel fault detection and classification index for active distribution network using differential components, *IEEE Trans. Ind. Appl.*, **60** (2024), 4530–4540. https://doi.org/10.1109/TIA.2024.3351617

29. M. Talaat, A. Y. Hatata, A. S. Alsayyari, A. Alblawi, A smart load management system based on the grasshopper optimization algorithm using the under-frequency load shedding approach, *Energy*, **190** (2020), 116423. https://doi.org/10.1016/j.energy.2019.116423

30. I. Laamanen, S. Repo, T. Stetz, Active network management integration in expansion planning of active distribution networks: a comprehensive review, *IEEE Access*, **14** (2026), 4520–4549. https://doi.org/10.1109/ACCESS.2025.3650636

31. T. Liu, J. Li, X. Zhang, D. Zhang, C. Hu, K. Feng, et al., Optimization of high-frequency transmission line reflection wave compensation and impedance matching based on a DQN-GA hybrid algorithm, *Electronics*, **15** (2026), 645. https://doi.org/10.3390/electronics15030645

32. S. K. Rathor, D. Saxena, Energy management system for smart grid: an overview and key issues, *Int. J. Energy Res.*, **44** (2020), 4067–4109. https://doi.org/10.1002/er.4883

33. C. Gu, J. Wang, L. Wu, Distributed energy resource and energy storage investment for enhancing flexibility under a TSO-DSO coordination framework, *IEEE Trans. Autom. Sci. Eng.*, **21** (2024), 2961–2973. https://doi.org/10.1109/TASE.2023.3272532

34. M. A. Kamarposhti, R. Ghandour, M. Abdel-Aty, M. Hafez, M. Alfiras, S. Alkhazaleh, et al., Optimizing capacitor bank placement in distribution networks using a multi-objective particle swarm optimization approach for energy efficiency and cost reduction, *Sci. Rep.*, **15** (2025), 12332. https://doi.org/10.1038/s41598-025-96341-8

35. Z. Yao, X. Liang, G. P. Jiang, J. Yao, Model-based reinforcement learning control of electrohydraulic position servo systems, *IEEE/ASME Trans. Mech.*, **28** (2023), 1446–1455. https://doi.org/10.1109/TMECH.2022.3219115

36. Z. Yao, X. Liang, S. Wang, J. Yao, Model-data hybrid driven control of hydraulic Euler–Lagrange systems, *IEEE/ASME Trans. Mech.*, **30** (2025), 131–143. https://doi.org/10.1109/TMECH.2024.3390129

37. C. Bariya, Optimal power flow using hybrid metaheuristic algorithms with RES and EV integration, *Turkish J. Eng.*, **10** (2026), 676–688. https://doi.org/10.31127/tuje.1840309

38. A. H. Adam, S. Kamel, M. H. Hassan, G. I. Mustafa, Optimal power flow of hybrid wind/solar/thermal energy integrated power systems considering renewable energy uncertainty via an enhanced weighted mean of vectors algorithm, *PLOS One*, **21** (2026), e0336157. https://doi.org/10.1371/journal.pone.0336157

39. H. M. Sultan, A. A. Z. Diab, A. S. Menesy, M. Kassas, M. Alqahtani, M. Khalid, et al., Enhancing optimal power flow in power systems: a comparative analysis of recent metaheuristic optimization techniques, *Energy Rep.*, **13** (2025), 3957–3999. https://doi.org/10.1016/j.egyr.2025.03.031

40. J. Liu, Z. Hou, B. Wang, T. Yin, Optimizing microgrid energy management via DE-HHO hybrid metaheuristics, *Comput. Mater. Continua*, **84** (2025), 4729–4754. https://doi.org/10.32604/cmc.2025.066138

41. S. Yin, M. S. Nazeer, M. Amin, K. Ullah, Z. Ali, Y. Shang, et al., A robust intuitionistic fuzzy framework for optimizing emergency response strategies under uncertain disaster risk conditions, *Ain Shams Eng. J.*, **17** (2026), 103883. https://doi.org/10.1016/j.asej.2025.103883

42. J. H. Zhu, J. S. Wang, X. Y. Zhang, Y. C. Wang, H. M. Song, Y. Zheng, et al., Multi-objective coyote optimization algorithm based on hybrid elite framework and Meta-Lamarckian learning strategy for optimal power flow problem, *Artif. Intell. Rev.*, **57** (2024), 117. https://doi.org/10.1007/s10462-024-10752-z

43. M. S. Shaikh, H. Lin, S. Xie, X. Dong, Y. Lin, C. K. Shiva, et al., An intelligent hybrid grey wolf-particle swarm optimizer for optimization in complex engineering design problem, *Sci. Rep.*, **15** (2025), 18313. https://doi.org/10.1038/s41598-025-02154-0

44. M. Al-Kaabi, V. Dumbrava, M. Eremia, Multi criteria frameworks using new meta-heuristic optimization techniques for solving multi-objective optimal power flow problems, *Energies*, **17** (2024), 2209. https://doi.org/10.3390/en17092209

45. I. Ahmed, U. E. H. Alvi, A. Basit, T. Khursheed, A. Alvi, K. S. Hong, et al., A novel hybrid soft computing optimization framework for the dynamic economic dispatch problem of complex non-convex contiguous constrained machines, *PLOS One*, **17** (2022), e0261709. https://doi.org/10.1371/journal.pone.0261709

Appendix

Theoretical convergence analysis

Theorem 1. Probabilistic convergence of the proposed TAHO algorithm. Let $\Omega \subset \mathbb{R}^D$ be a nonempty, closed, and bounded feasible search space of the OPF problem, and let $f\colon \Omega \to \mathbb{R}$ be the normalized multi-objective fitness function. Assume that f is bounded below and has at least one global optimum $X^* \in \Omega$. If the proposed TAHO algorithm satisfies the following conditions:

(1) The population is initialized inside the feasible search space Ω;
(2) All candidate solutions are repaired or projected back into Ω after each update;
(3) The stochastic PSO, GWO, and JS search operators have a nonzero probability of generating a candidate solution in any neighborhood of X^*;
(4) The best-so-far solution is preserved using an elitist selection rule;

then the best fitness value generated by TAHO converges to the global optimum with probability one, i.e.,

$$P\left(\lim_{t\to\infty} f(gbest^t) = f(X^*)\right) = 1.$$

Proof. Let the population state of TAHO at iteration t be defined as

$$S_t = \{X_1^t, X_2^t, \ldots, X_N^t, gbest^t\},$$

where X_i^t is the ith candidate solution, N is the population size, and $gbest^t$ is the best-so-far solution obtained up to iteration t. Since the next population state S_{t+1} is generated from the current state S_t, random coefficients, and adaptive weights α_t, β_t, and γ_t, the transition of the algorithm satisfies the Markov property:

$$P(S_{t+1} \mid S_t, S_{t-1}, \ldots, S_0) = P(S_{t+1} \mid S_t).$$

Therefore, the TAHO search process can be modeled as a Markov chain over the feasible search space Ω. For any $\epsilon > 0$, define the ϵ-optimal region as

$$\Omega_\epsilon = \{X \in \Omega : f(X) - f(X^*) < \epsilon\}.$$

Since the PSO, GWO, and JS operators are stochastic and the JS component preserves population diversity, there exists a constant $\delta > 0$ such that

$$P(S_{t+1} \cap \Omega_\epsilon \neq \emptyset \mid S_t) \geq \delta.$$

This means that, from any current population state, the probability of generating at least one solution inside the ϵ-optimal region is nonzero. The probability that the population does not visit Ω_ϵ during the first T iterations is therefore bounded by

$$P(S_t \cap \Omega_\epsilon = \emptyset,\ t = 1, 2, \ldots, T) \leq (1 - \delta)^T.$$

Taking the limit as $T \to \infty$ gives

$$\lim_{T\to\infty}(1-\delta)^T = 0.$$

Hence,

$$P(\exists t : S_t \cap \Omega_\epsilon \neq \emptyset) = 1.$$

Therefore, the population reaches the ϵ-optimal region with probability one. The proposed TAHO algorithm applies elitist best-solution preservation. Hence, the best fitness sequence satisfies

$$f(gbest^{t+1}) \leq f(gbest^t).$$

Thus, $\{f(gbest^t)\}$ is monotonically non-increasing. Since f is bounded below by the global optimum $f(X^*)$, we have

$$f(gbest^t) \geq f(X^*), \quad \forall t.$$

Therefore, by the monotone convergence theorem, the sequence $\{f(gbest^t)\}$ converges to a finite limit. Since the population enters every ϵ-optimal region with probability one and the best-so-far solution is never discarded, the limiting value of the best fitness sequence must satisfy

$$\lim_{t\to\infty} f(gbest^t) \leq f(X^*) + \epsilon.$$

Because $\epsilon > 0$ is arbitrary, it follows that

$$\lim_{t\to\infty} f(gbest^t) = f(X^*)$$

with probability one. Therefore,

$$P\left(\lim_{t\to\infty} f(gbest^t) = f(X^*)\right) = 1.$$

This proves that the proposed TAHO algorithm probabilistically converges to the global optimum under the stated assumptions. □

AIMS Press